Compressive Response Determination of Closed-Cell Aluminium Foam and Linear-Elastic Finite Element Simulation of µCT-Based Directly Reconstructed Geometrical Models

Tamás Mankovits[1],* – Tamás Antal Varga[1] – Sándor Manó[2] – Imre Kocsis[1]

[1] University of Debrecen, Faculty of Engineering, Hungary
[2] University of Debrecen, Faculty of Medicine, Hungary

The development of an efficient procedure for three-dimensional modelling and finite element simulation of metal foams remains one of the greatest challenges for engineers. The numerical determination of compressive properties of foam structure is a demanding engineering task and is indispensable for design purposes. In the design of load-bearing metal foam structures, the elastic behaviour under working circumstances must be considered and for the engineering calculations on the actual foam structure its precise geometrical modelling is necessary. Closed-cell aluminium foam produced from Duralcan F3.S.20S metal matrix composite (MMC) and fabricated by direct foaming technique is analysed. To ensure full comparability, specimens are characterized according to the ruling standard for compression test for porous materials. In this paper, a manual geometrical reconstruction process based on evaluation of images given by X-ray computed tomography and the related finite element calculations is introduced. The proposed procedure is capable of investigating the actual structure as a three-dimensional problem from any kind of material that can be analysed on the basis of computed tomography (CT) images. The geometrical reconstruction and the finite element calculation results show good correlation with the measured values in the elastic, which proves the utility of the presented method.
Keywords: closed-cell foam, geometrical reconstruction, compression test, finite element method

Highlights
- *Foam structure produced from Duralcan F3.S20S MMC is analysed experimentally and numerically.*
- *Manual geometric reconstruction of closed-cell foam structures is presented.*
- *Finite element calculations of the actual geometry of foam structures are executed.*
- *Calculations based on geometrical model precisely described the compressive response in the elastic region.*

0 INTRODUCTION

Metal foams have a lightweight cellular structure with excellent mechanical and physical properties. It is well known that metal foams have high compression strength combined with good energy absorption characteristics [1]. Therefore, the interest in these materials is widespread not only as a vibration damper or sound absorber but also as a load-bearing structural element. Numerous applications rely on the compressive property of metal foams, which directly depend on its structure. As a load-bearing structural element (e.g. vehicle part, biomedical implant) metal foam is expected to behave elastically under working circumstances, so the material response must be predicted precisely in the elastic region. Numerical determination of compressive properties of foam structure remains a demanding engineering task, and it is indispensable for design purposes.

A number of studies have reported on measuring the material response of different types of metal foams in destructive ways. The compressive properties of open cell metal foams in [2] and [3], metal matrix syntactic foams in [4] to [8], and titanium foam in

[9] were investigated, while the elastic behaviour of closed-cell aluminium foam under uniaxial loading and bending conditions was also studied in [10].

Geometrical modelling is an essential part of the procedure aiming the investigation of metal foam structures in a numerical way. Numerous approaches can be found in the literature for the proper description of foam structures, one of which is the usage of uniform cell models which results in simplified geometry compared with the actual structure. A combination of spherical and cruciform-shaped cells was used to model closed-cell aluminium foam and to simulate its material response in [11], while different uniform cell structures were applied to the model and simulate open cell metal foams in [12] to [14]. Diamond and cubic cell foam structure were also used to simulate the effect of cell shape on the mechanical behaviour of open cell metal foams in [15].

Since the inner structure of different types of metal foams is quite complicated, a surface analysis can result in imperfect or false data. Recent studies proved X-ray computed tomography to be an efficient and powerful tool for mapping the complete structure

of materials in a non-invasive and non-destructive way.

The development of a mesoscale simulation modelling voids and sintered hollow spheres as a metal foam structure was presented in [16]. 3D models of microporous ceramics were generated, and the determination of the porosity was studied in [17]. Two-dimensional models based on μCT images were established to investigate mechanical properties of different foam structures in [18] to [24]. An overview of the auxetic cellular materials was presented in [25].

A new CAD modelling procedure applied to a circular foam billet was proposed, and the structure was obtained, introducing spherical surfaces, which represented the internal voids of an aluminium foam in [26]. The linear elastic properties were determined by the usage of finite element method based on random tessellations for the generation of microstructure in [27], and geometrical reconstruction processes of open cell foam structures were investigated in [28] and [29]. Randomly shaped Voronoi polyhedrals were used to form the pore network of open cell titanium foam and finite element prediction of the compressive characteristics was presented in [30]. A finite element model was introduced for the determination of mechanical properties of non-uniform cellular aluminium in [31]. A random number generator was established to model the proper distribution of the hollow spheres, and finite element simulation was performed to determine the compressive material response of metal matrix syntactic foams in [32]. Syntactic foam structure was analysed and the three-dimensional CAD model was established in [33]. Three mesh generating methods (Voronoi description of the microstructure, voxel meshes, and tetrahedral meshes) using tomographic images of the actual shape of cellular structures were investigated in [34]. The exact geometrical data of single sintered metallic hollow spheres were obtained by CT scanning, and the corresponding finite element models were created in [35]. Advanced pore morphology (APM) foam elements were investigated and compressive force-displacement response was evaluated numerically in [36].

Three-dimensional models were generated based on μCT images and numerical calculations were performed on cellular structures in [37] and [38]. The local deformation mechanisms of the actual foam structure during compression were investigated using different mesh size discretizations in [39]. Closed-cell aluminium foams in [40] and [41] and open cell aluminium foams in [42] to [44] were investigated numerically based on μCT images and the material

response for compression was determined. The deformation and plastic collapse mechanisms of closed-cell aluminium foams were analysed with finite element method based on μCT. The geometrical reconstruction was performed with software RapidForm™ in [45]. The 3D geometry of closed-cell aluminium foam derived from the synthesis of digital cross-section images was used to build the finite element model simulating the deformation conditions of the foam under micro-tension loads and compression in [46] and [47]. The strain rate-dependent compression response of Ni-foam was determined by the finite element method based on μCT images in [48]. A novel reconstruction method with Matlab image processing and CT scanning was applied and the finite element method was used to determine the thermal conductivity and the material response of a closed-cell aluminium foam in [49] and [50].

The number of publications in the field of geometrical modelling and finite element analysis of metal foam structures demonstrates that this topic is in the focus of studies. To obtain high-quality predictions of a porous material response, it is critical to constructing FEM models that provide an adequate description of the actual geometry. In this research, a geometrical reconstruction of closed-cell aluminium foam and finite element analysis of the structure in the elastic region is presented. The deviation between the simulation and measurement results is not significant, proving that the method is suitable for the description of real structures.

An essential part of the procedure is a manual reconstruction method for objects of complex geometry. The first step is the preparation of plane sections (CT images) with parallel planes of given density. The second is the performance of a series of transformations providing a geometrically accurate three-dimensional object that is suitable for finite element analysis. The investigation of specimens proves that the accuracy of the proposed reconstruction method meets the requirements and the procedure can be reproduced and validated.

1 MATERIALS AND EXPERIMENTAL METHODS

The examined closed-cell aluminium foam was produced from Duralcan F3S.20S Metal Matrix Composite and fabricated using a direct foaming technique by adding blowing agent. Considering the finite element investigations, the relevant physical and mechanical properties of the solid phase were measured [51]. The chemical composition was also evaluated with EDX analysis and compared with the

data available in the literature. The density of the raw material was measured. The SiC median particle size was determined by microscopic analysis using a Hitachi Tabletop 3030 SEM microscope. According to the ASTM E9-09 standard [52], the modulus of elasticity was evaluated by compression test using an INSTRON 8874 testing machine. The diameter and the length of the solid specimens were 13 mm and 25 mm, respectively. The measuring results listed in Table 1 showed good conformity with the commercial data. Several physical and mechanical properties of the three specimens were investigated. According to the measurement data, porosity of pieces showed low variability.

Table 1. *Chemical composition and related physical and mechanical properties of the applied matrix material*

Main components	Commercial and literature data [53]	Measured data
Al [wt%]	68.53	69.26
Si [wt%]	9.3	9.21
Mg [wt%]	0.55	0.53
SiC [wt%]	21.4	20.8
other [wt%]	0.22	0.2
Properties		
SiC median particle size [mm]	12.8	13.24
Density [kg/m³]	2850	2875.12
Modulus of elasticity [GPa]	98.6	97.2

The size of the specimens was determined according to the ISO 13314 standard on the basis of a statistical analysis of the pore sizes. Similar investigations were published in [51] by the authors. The size of the specimens was 14.5 mm × 14.5 mm × 14.5 mm (see Fig. 1); STRUERS Labotom-15 was used for cutting.
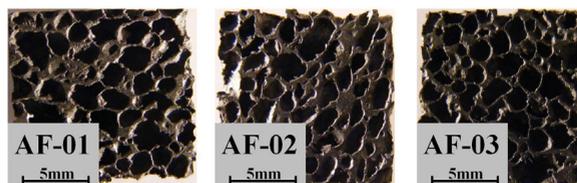
Fig. 1. *Closed-cell aluminium foam specimens*

The compression tests were performed on an INSTRON 8874 type universal testing machine at room temperature. The compression tests were carried out with the application of lubricant. The deformation rate was maintained in quasi-static condition at 8.7 mm/min. During the tests, the engineering stress-engineering strain curves were registered and processed according to the ruling standard for the compression test for porous and cellular materials [54].

The basis of the geometrical reconstruction was the microcomputed-tomography analysis that was performed using a YXILON CT Modular type industrial CT equipment with X-ray tube of 225 kV and resolution of 7 mm.

Using Materialise Mimics v10.1 and its complement Materialise Magics v9.9, the reconstruction of the geometry of the samples were established through some manual steps. The automatic reconstruction was compared with the manual reconstruction process, and the results of the proposed process were qualified. An evaluation copy of VGStudio Max 3.0 was used to control the quality of the geometric reconstruction; the original structure was compared with the reconstructed one. The finite element calculations with Femap 9.3 was used to generate load-displacement curves in the elastic region. The results showed excellent correlation with the compression tests.

2 RESULTS AND DISCUSSION

2.1 Compressive Properties

The compressive properties of the three aluminium foam specimens were determined at a constant loading speed of 8.7 mm/min according to the standard [54]. The standard introduces several important terms to evaluate the behaviour and compressive properties of metal foams and cellular metallic materials. The most important ones are plateau stress (average stress between 20 % and 40 % compressive strain); quasi-
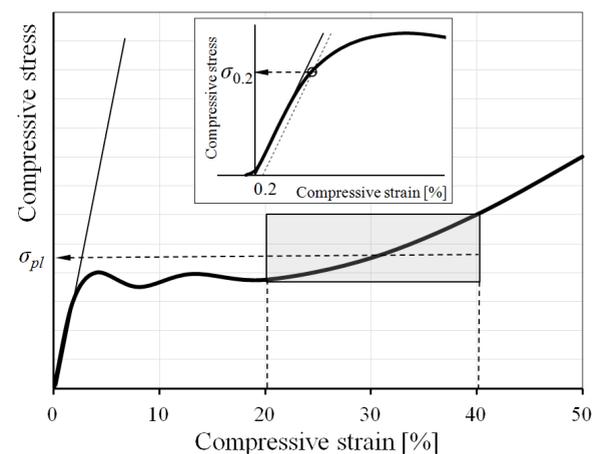
Fig. 2. *Determination of the plateau stress (σpl), the quasi-elastic gradient and the compressive offset stress (σ0.2) based on ISO 13314:2011*

elastic gradient (gradient of the straight line within the linear deformation region at the beginning of the compressive stress-strain curve); compressive offset stress (compressive stress at the plastic compressive strain of 0.2 %), see Fig. 2.

The compressive stress-strain curve of the investigated specimens can be seen in Fig. 3. The compressive offset stress, the quasi-elastic gradient and the plateau stress were calculated from the compressive stress-strain curves.
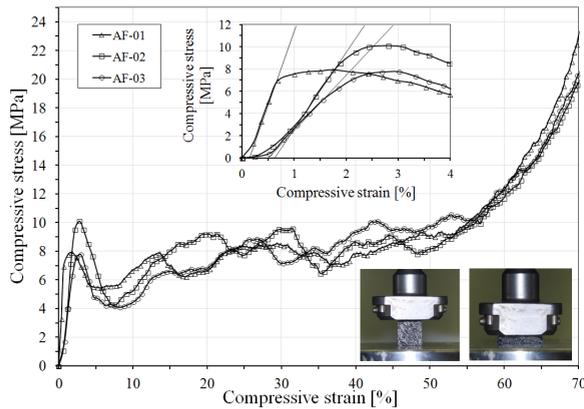
Fig. 3. *Compressive stress-strain curve of foam specimens*

The results of the compression tests are listed in Table 2.

Table 2. *Compressive properties of the aluminium foam specimens*

Compressive properties	AF-01	AF-02	AF-03
Compressive offset stress [MPa]	7.434	9.760	7.332
Quasi-elastic gradient [MPa]	1295	738.9	500.5
Plateau stress [MPa]	7.757	8.085	8.355

Table 2 shows that significant deviation of plateau stresses cannot be observed, while the elastic properties (compressive offset stress and quasi-elastic gradient) are different. Considering the specific structure of the closed-cell metal foams, it can be supposed that the elastic properties primarily depend on the porosity, the distribution of the cell volume (described by quartiles, Q_1, Q_2, Q_3), the sum of the cell volumes in the failure zone (V_C) and the area of the surfaces (A_C) contacting the compression plates. The porosity evaluation was based on weight and volume measurements. Foam structure analysis was carried out with VGStudio Max 3.0, and the extents of the contact surface were determined by image processing analysis. The measurement results are listed in Table 3. During the compression test, it is obtained that the failure starts in the middle section of the specimens.

Table 3. *Structural properties of the aluminium foam specimens*

	AF-01	AF-02	AF-03
Porosity [%]	85.16	85.4	85.38
Mass [g]	1.33	1.36	1.34
Q_1	0.28	0.35	0.31
Q_2	0.72	0.91	0.82
Q_3	1.94	2.12	2.24
V_C [mm³]	211.93	189.64	204.45
A_C [%]	41.39	47.48	50.27

According to Table 3, the structural properties of the aluminium foam, depending on the manufacturing technology, show no significant deviation, while the extent of contact surfaces is highly influenced by the position of the cutting planes. Furthermore, a significant variance can be detected in the sum cell volumes in the failure zone. Because of the deviation of the elastic properties (Fig. 3), a finite element analysis is necessary in the elastic sector. According to our investigations, the extent of the contact surfaces and the elastic properties seem to be related, but further research is necessary to obtain a more precise connection.

2.2 Geometrical Reconstruction Process

The basis of the procedure is a series of CT images in DICOM format that is converted into an image stack, the input of the software that provides the structure in STL format. Transformations of this structure yield a format (IGES, NAS, etc.) that is suitable for further engineering calculations.

The accuracy of the finite element calculations highly depends on the deviation between the original and the reconstructed geometry.

Finding the connecting points of cell walls requires sharp contours between phases in section images. The contours in CT images used in the investigation can be detected with high accuracy, but the images contain noise because of the imaging technique.

The accuracy of the reconstruction also depends on the distance between slicing planes, which affects the minimum level of the detectable cell size and on the complexity of cell wall surfaces (a non-smooth surface and a deviation from sphere reduce the accuracy of the reconstruction).

Materialise Mimics v10.1 is used for the reconstruction process; this software allows the automatic reconstruction, which results in a model that is suitable for finite element analysis, but the accuracy of the geometrical conformity is not high

enough. Instead of an automatic reconstruction process, the software allows custom parameter setting defined by the user in each step of the transformation. The order of transformations can be chosen resulting in different model properties. The transformations provide STL files with different properties, e.g. mass, volume, number of elements. Fig. 4. shows the order of transformations that was proved to be the best for approximation in the modelling of closed-cell aluminium foams (the figure contains the original command names used in Mimics).

The five steps of the parameterized transformation resulted in 3.79×10^6, 3.58×10^6, 3.54×10^6 elements, while the automatic transformation led to a model of 9.10×10^6, 8.81×10^6, 6.88×10^6 elements, respectively. The total mass [g] after the parameterized transformation (1.3454, 1.3826, 1.3864) was close to the initial value (1.3509, 1.3762, 1.3660), while the total mass in the case of automatic reconstruction was 1.55, 1.53, 1.58, respectively, that is, significantly higher than the initial values.

The accuracy of geometry was checked by comparing the foam model provided by the reconstruction process with the model described by the STL file using the evaluation copy of VGStudio Max 3.0. The comparison resulted in a statistical evaluation of deviations. The regions where the deviation was significant were investigated to determine the accuracy of the given geometrical model. The ratio of surface values in the domain where the deviation between the initial and the transformed foam structure is greater than 0.02 mm is listed in Table 4.

Table 4. *Ratio of surface values where the deviation is greater than 0.02 mm*

	AF-01	AF-02	AF-03
Ratio [%] - automatic	1.703	1.293	1.290
Ratio [%] - parameterized	0.581	0.613	0.468

According to the analysis, the ratio of the surface where the deviation is greater than 0.02 mm was more than two times higher in the case of automatic reconstruction compared to the parameterized case. The image provided by the software enables the detailed investigation of high deviations. Fig. 5 shows a 2 mm × 2 mm × 2 mm size foam part; two details are highlighted where the two models differ.
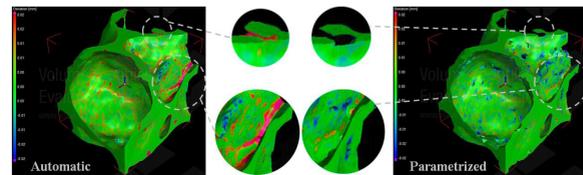
Fig. 5. *Detailed investigation using the images provided by the software*

Fig. 6 shows the complete modelling procedure in pictures: manufactured specimen, CT scanned image, image-stack, initial STL structure, reconstructed STL structure, meshed foam model and finite element evaluation. The benefit of the proposed procedure is the high precision preparation of the foam structure attained by the custom parameterized reconstruction method.
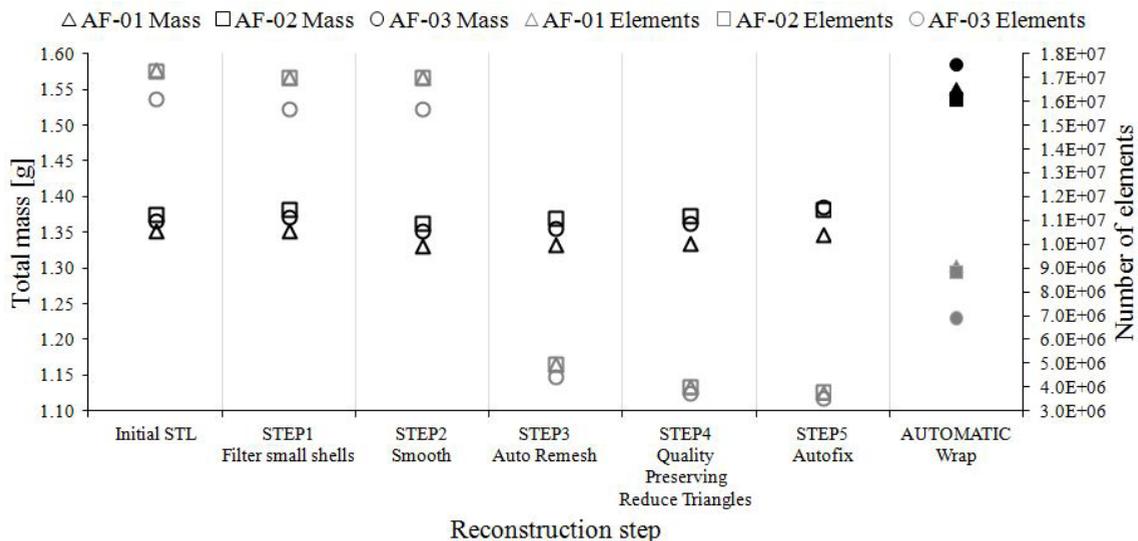
Fig. 4. *Comparison of the automatic and the parameterized processes (total volume, number of elements)*
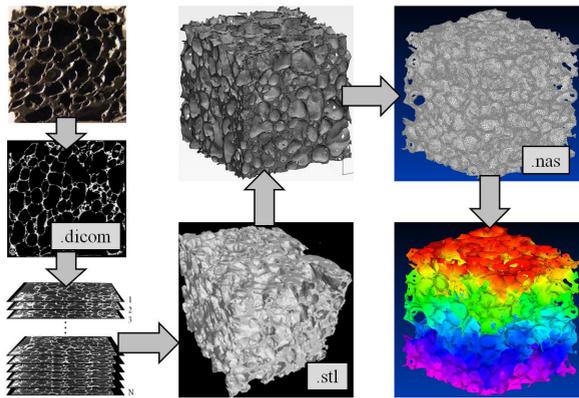
Fig. 6. *Complete modelling procedure*

2.3 Finite Element Calculations

The computational models were prepared to represent the experimental setup, and each consisted of an aluminium foam specimen and two rigid plates. Frictionless contact was assumed and used in the model. The rigid top plate had a prescribed displacement, and the bottom plate was fixed and used to measure the reaction force. The aluminium foam specimens were meshed with tetrahedron elements, and material properties were determined using experiments by the authors [51]. The properties of the finite element models are listed in Table 5. The computational models were analysed using the commercial finite element software Femap 9.3 with NX Nastran solver for quasi-static loading.

Table 5. *Properties of the finite element models*

	AF-01	AF-02	AF-03
Number of volume elements	6228541	5916312	5885768
Number of nodes	1852991	1759080	1744979
Largest volume element [mm³]	0.1661	0.05099	0.1342
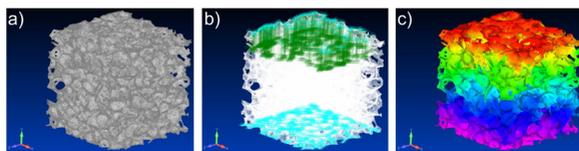
Fig. 7. *a) The meshed model, b) the boundary conditions, and c) the displacement state of a foam specimen*

The finite element settings and the simulation results are shown in Figs. 7 and 8 and listed in Table 6.

The finite element calculations correlated with the experimental results. For design purposes, the specification of the elastic behaviour of metal foam structural parts is indispensable. The finite element model can describe this feature on the basis of the accurate geometrical reconstruction.
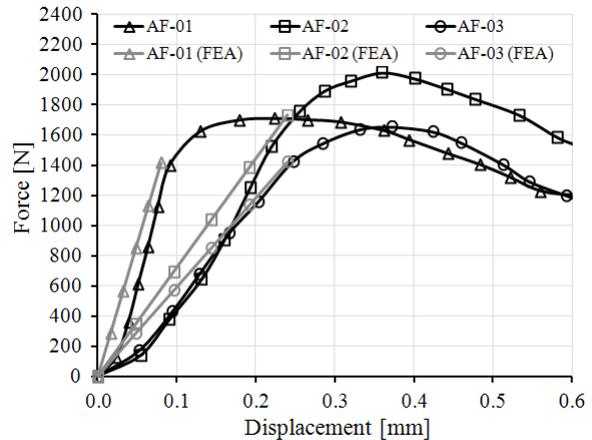
Fig. 8. *The real and the simulated force-displacement curves of the aluminium foam under quasi-static loading*

Table 6. *Comparison of the measured and simulated Quasi-elastic gradients in MPa*

	AF-01	AF-02	AF-03
Measurement	1295	738.9	500.5
Simulation	1243.4	689.7	476.3
Difference [%]	3.984	6.658	4.835

3 CONCLUSIONS

In the framework of the study, experimental and numerical analysis were conducted to clarify the elastic behaviour of metal foam. Closed-cell aluminium foams were compressed, and stress-strain curves were analysed. A deviation occurred in the elastic properties of foam specimens, which originated in the actual geometrical properties. For the numerical determination of elastic properties of the closed-cell aluminium foams, a manual geometrical reconstruction procedure was presented. This process was realized in several custom parameterized steps and resulted in a more accurate model than the automatic reconstruction used generally. The difference between the two procedures was proved with comparison analysis. The original image-stack was transformed into the form that is suitable for finite element simulations. The finite element calculations correlated with the experimental results and the numerical model precisely described the elastic behaviour of the investigated foam on the basis of the accurate geometrical reconstruction. The procedure can support the design process of load-bearing metal foam parts.

4 ACKNOWLEDGEMENTS

5 REFERENCES

[1] Ashby, M.F., Evans, A.G., Fleck, N.A., Gibson, L.J. (2000). *Metal Foams: A Design Guide*. Butterworth-Heinemann, Woburn.

[2] Devivier, C., Tagliaferri, V., Trovalusci, F., Ucciardello, N. (2015). Mechanical characterization of open cell aluminium foams reinforced by nickel electro-deposition. *Materials and Design*, vol. 86, p. 272-278, **DOI:10.1016/j.matdes.2015.07.078**.

[3] Xiao, L., Song, W., Tang, H., Zhu, Z., Wang, J., Wang, H. (2015). High temperature compression properties of open-cell Ni–20Cr foams produced by impregnation. *Materials and Design*, vol. 85, p. 47-53, **DOI:10.1016/j.matdes.2015.06.167**.

[4] Orbulov, I.N., Májlinger, K. (2013). Description of the compressive response of metal matrix syntactic foams. *Materials and Design*, vol. 49, p. 1-9, **DOI:10.1016/j.matdes.2013.02.007**.

[5] Orbulov, I.N. (2012). Compressive properties of aluminium matrix syntactic foams. *Materials Science and Engineering: A*, vol. 555, p. 52-56, **DOI:10.1016/j.msea.2012.06.032**.

[6] Peroni, L., Scapin, M., Avalle, M., Weise, J., Lehmhus, D., Baumeister, J., Busse, M. (2012). Syntactic iron foams – on deformation mechanisms and strain-rate dependence of compressive properties. *Advanced Engineering Materials*, vol. 14, no. 10, p. 909-918, **DOI:10.1002/adem.201200160**.

[7] Luong, D.D., Shunmugasamy, V.C., Gupta, N., Lehmhus, D., Weise, J., Baumeister, J. (2015). Quasi-static and high strain rates compressive response of iron and Invar matrix syntactic foams. *Materials and Design*, vol. 66, part B, p. 516-531, **DOI:10.1016/j.matdes.2014.07.030**.

[8] Peroni, L., Scapin, M., Fichera, C., Lehmhus, D., Weise, J., Baumeister, J., Avalle, M. (2014). Investigation of the mechanical behaviour of AISI 316L stainless steel syntactic foams at different strain-rates. *Composites Part B: Engineering*, vol. 66, p. 430-442, **DOI:10.1016/j.compositesb.2014.06.001**.

[9] Pałka, K., Adamek, G., Jakubowicz, J. (2016). Compression behavior of Ti Foams with spherical and polyhedral pores. *Advanced Engineering Materials*, vol. 18, no. 8, p. 1511-1518, **DOI:10.1002/adem.201600169**.

[10] Triawan, F., Kishimoto, K., Adachi, T., Inaba, K., Nakamura, T., Hashimura, T. (2012). The elastic behavior of aluminum alloy foam under uniaxial loading and bending conditions. *Acta Materialia*, vol. 60, no. 6-7, p. 3084-3093, **DOI:10.1016/j.actamat.2012.02.013**.

[11] Hasan, A. (2010). An improved model for FE modeling and simulation of closed cell Al-alloy foams. *Advances in Materials Science and Engineering*, article ID 567390, **DOI:10.1155/2010/567390**.

[12] Kou, D.P., Li, J.R., Yu, J.L., Cheng, H.F. (2008). Mechanical behavior of open-cell metallic foams with dual-size cellular structure. *Scripta Materialia*, vol. 59, no. 5, p. 483-486, **DOI:10.1016/j.scriptamat.2008.04.022**.

[13] Jang, W.Y., Kyriakides, S., Kraynik, A.M. (2010). On the compressive strength of open-cell metal foams with Kelvin and random cell structures. *International Journal of Solids and Structures*, vol. 47, no. 21, p. 2872-2883, **DOI:10.1016/j.ijsolstr.2010.06.014**.

[14] Lu, Z.X., Liu, Q., Huang, J.X. (2011). Analysis of defects on the compressive behaviors of open-cell metal foams through models using the FEM. *Materials Science and Engineering: A*, vol. 530, p. 285-296, **DOI:10.1016/j.msea.2011.09.088**.

[15] An, Y., Wen, C., Hodgson, P.D., Yang, C. (2012). Investigation of cell shape effect on the mechanical behaviour of open-cell metal foams. *Computational Materials Science*, vol. 55, p. 1-9, **DOI:10.1016/j.commatsci.2011.11.030**.

[16] Smith, B.H., Szyniszewski, S., Hajjar, J.F., Schafer, B.W., Arwade, S.R. (2012). Characterization of steel foams for structural components. *Metals*, vol. 2, no. 4, p. 399-410, **DOI:10.3390/met2040399**.

[17] Schmidt, K., Becker, J. (2012). Generating validated 3D models of microporous ceramics. *Advanced Engineering Materials*, vol. 15, no. 1-2, p. 40-45, **DOI:10.1002/adem.201200097**.

[18] Shen, H., Brinson, L.C. (2007). Finite element modeling of porous titanium. International *Journal of Solids and Structures*, vol. 44, no. 1, p. 320-335, **DOI:10.1016/j.ijsolstr.2006.04.020**.

[19] Kádár, Cs., Maire, E., Borbély, A., Peix, G., Lendvai, J., Rajkovits, Zs. (2004). X-ray tomography and finite element simulation of the indentitation behavior of metal foams. *Materials Science and Engineering: A*, vol. 387-389, p. 321-325, **DOI:10.1016/j.msea.2004.03.091**.

[20] Zhu, X., Ai, S., Fang, D., Liu, B., Lu, X. (2014). A novel modeling approach of aluminum foam based on MATLAB image processing. *Computational Materials Science*, vol. 82, p. 451-456, **DOI:10.1016/j.commatsci.2013.10.020**.

[21] Adziman, M.F., Deshpande, S., Omiya, M., Inoue, H., Kishimoto, K. (2007). Compressive deformation in aluminum foam investigated using a 2D object oriented finite element modeling approach. *Key Engineering Materials*, vol. 353-358, p. 651-654, **DOI:10.4028/www.scientific.net/KEM.353-358.651**.

[22] Vendra, L., Rabiei, A. (2010). Evaluation of modulus of elasticity of composite metal foams by experimental and numerical techniques. *Materials Science and Engineering: A*, vol. 527, no. 7-8, p. 1784-1790, **DOI:10.1016/j.msea.2009.11.004**.

[23] Caty, O., Maire, E., Youssef, S., Bouchet, R. (2008). Modeling the properties of closed-cell cellular materials from tomography images using finite shell elements. *Acta Materialia*, vol. 56, no. 19, p. 5524-5534, **DOI:10.1016/j.actamat.2008.07.023**.

[24] Storm, J., Abendroth, M., Emmel, M., Liedke, T., Ballaschk, U., Voigt, C., Sieber, T., Kuna, M. (2013). Geometrical modelling of foam structures using implicit functions. *International Journal of Solids and Structures*, vol. 50, no. 3-4, p. 548-555, **DOI:10.1016/j.ijsolstr.2012.10.026**.

[25] Novak, N., Vesenjak, M., Ren, Z. (2016). Auxetic cellular materials – a Review. *Strojniski vestnik – Journal of Mechanical Engineering*, vol. 62, no. 9, p. 485-493, **DOI:10.5545/sv-jme.2016.3656**.

[26] Filice, L., Gagliardi, F., Umbrello, D. (2009). Simulation of aluminum foam behavior in compression tests. *The Arabian Journal for Science and Engineering*, vol. 34, no. 1C, p. 129-137.

[27] Geißendörfer, M., Liebscher, A., Proppe, C., Redenbach, C., Schwarzer, D. (2014). Stochastic multiscale modeling of metal foams. *Probabilistic Engineering Mechanics*, vol. 37, p. 132-137, **DOI:10.1016/j.probengmech.2014.06.006**.

[28] Vesenjak, M., Veyhl, C., Fiedler, T. (2012). Analysis of anisotropy and strain rate sensitivity of open-cell metal foam. *Materials Science and Engineering: A*, vol. 541, p. 105-109, **DOI:10.1016/j.msea.2012.02.010**.

[29] Zhang, T., Maire, E., Adrien, J., Onck, P.R., Salvo, L. (2013). Local tomography study of the fracture of an ERG metal foam. *Advanced Engineering Materials*, vol. 15, no. 8, p. 767-772, **DOI:10.1002/adem.201300004**.

[30] Siegkas, P., Tagarielli, V., Petrinic, N. (2014). Modelling stochastic foam geometries for FE simulations using 3D Voronoi cells. *Procedia Materials Science*, vol. 4, p. 221-226, **DOI:10.1016/j.mspro.2014.07.604**.

[31] Foroughi, B., Degischer, H.P., Kottar, A. (2013). Characterization and simulation of tensile deformation of non-uniform cellular aluminium until damage. *Advanced Engineering Materials*, vol. 15, no. 4, p. 276-286, **DOI:10.1002/adem.201200163**.

[32] Szlancsik, A., Katona, B., Bobor, K., Májlinger, K., Orbulov, I.N. (2015). Compressive behaviour of aluminium matrix syntactic foams reinforced by iron hollow spheres. *Materials and Design*, vol. 83, p. 230-237, **DOI:10.1016/j.matdes.2015.06.011**.

[33] Kozma, I., Zsoldos, I., Dorogi, G., Papp, S. (2014). Computer tomography based reconstruction of metal matrix syntactic foams. *Periodica Polytechnica Mechanical Engineering*, vol. 58, no. 2, p. 87-91, **DOI:10.3311/PPme.7337**.

[34] Maire, E., Fazekas, A., Salvo, L., Dendievel, R., Youssef, S., Cloetens, P., Letang, J.M. (2003). X-ray tomography applied to the characterization of cellular materials. Related finite element modeling problems. *Composites Science and Technology*, vol. 63, no. 16, p. 2431-2443, **DOI:10.1016/S0266-3538(03)00276-8**.

[35] Borovinšek, M., Vesenjak, M., Ren, Z. (2016). Estimating the base material properties of sintered metallic hollow spheres by inverse engineering procedure. *Mechanics of Materials*, vol. 100, p. 22-30, **DOI:10.1016/j.mechmat.2016.06.001**.

[36] Sulong, M.A., Vesenjak, M., Belova, I.V., Murch, G.E., Fiedler, T. (2014). Compressive properties of Advanced Pore Morphology (APM) foam elements. *Materials Science and Engineering: A*, vol. 607, p. 498-504, **DOI:10.1016/j.msea.2014.04.037**.

[37] Doroszko, M., Seweryn, A. (2015). Numerical modeling of the tensile deformation process of sintered 316L based on microtomography of porous mesostructures. *Materials and Design*, vol. 88, p. 493-504, **DOI:10.1016/j.matdes.2015.09.006**.

[38] Jirousek, O., Doktor, T., Kytýř, D., Zlámal, P., Fíla, T., Koudelka, P., Jandejsek, I., Vavřík, D. (2013). X-ray and finite element analysis of deformation response of closed-cell metal foam subjected to compressive loading. *Journal of Instrumentation*, vol. 8, p. 1-4, **DOI:10.1088/1748-0221/8/02/C02012**.

[39] Youssef, S., Maire, E., Gaertner, R. (2005). Finite element modelling of the actual structure of cellular materials determined by X-ray tomography. *Acta Materialia*, vol. 53, no. 3, p. 719-730, **DOI:10.1016/j.actamat.2004.10.024**.

[40] Saadatfar, M., Mukherjee, M., Madadi, M., Schröder-Turk, G.E., Garcia-Moreno, F., Schaller, F.M., Hutzler, S., Sheppard, A.P., Banhart, J., Ramamurty, U. (2012). Structure and deformation correlation of closed-cell aluminium foam subject to uniaxial compression. *Acta Materialia*, vol. 60, no. 8, p. 3604-3615, **DOI:10.1016/j.actamat.2012.02.029**.

[41] Hangai, Y., Yamaguchi, R., Takahashi, S., Utsunomiya, T., Kuwazuru, O., Yoshikawa, N. (2013). Deformation behavior estimation of aluminum foam by X-ray CT image-based finite element analysis. *Metallurgical and Materials Transactions: A*, vol. 44, no. 4, p. 1880-1887, **DOI:10.1007/s11661-012-1532-7**.

[42] Veyhl, C., Belova, I.V., Murch, G.E., Fiedler, T. (2011). Finite element analysis of the mechanical properties of cellular aluminium based on micro-computed tomography. *Materials Science and Engineering: A*, vol. 528, no. 13-14, p. 4550-4555, **DOI:10.1016/j.msea.2011.02.031**.

[43] Michailidis, N., Stergioudi, F., Omar, H., Papadoupoulos, D., Tsipas, D.N. (2011). Experimental and FEM analysis of the material response of porous metals imposed to mechanical loading. *Colloids and Surfaces A: Physicochemical and Engineering Aspects*, vol. 382, no. 1-3, p. 124-131, **DOI:10.1016/j.colsurfa.2010.12.017**.

[44] Ramírez, J.F., Cardona, M., Velez, J.A., Mariaka, I., Isaza, J.A., Mendoza, E., Betancourt, S., Fernández-Morales, P. (2014). Numerical modeling and simulation of uniaxial compression of aluminum foams using FEM and 3D-CT images. *Procedia Materials Science*, vol. 4, p. 227-231, **DOI:10.1016/j.mspro.2014.07.609**.

[45] Jeon, I., Asahina, T., Kang, K.J., Im, S., Lu, T.J. (2010). Finite element simulation of the plastic collapse of closed-cell aluminum foams with X-ray computed tomography. *Mechanics of Materials*, vol. 42, no. 3, p. 227-236, **DOI:10.1016/j.mechmat.2010.01.003**.

[46] Michailidis, N., Stergioudi, F., Omar, H., Tsipas, D.N. (2010). An image-based reconstruction of the 3D geometry of an Al open-cell foam and FEM modeling of the material response. *Mechanics of Materials*, vol. 42, no. 2, p. 142-147, **DOI:10.1016/j.mechmat.2009.10.006**.

[47] Michailidis, N., Stergioudi, F., Omar, H., Tsipas, D.N. (2010). FEM modeling of the response of porous Al in compression. *Computational Materials Science*, vol. 48, no. 2, p. 282-286, **DOI:10.1016/j.commatsci.2010.01.008**.

[48] Michailidis, N. (2011). Strain rate dependent compression response of Ni-foam investigated by experimental and FEM simulation methods. *Materials Science and Engineering: A*, vol. 528, no. 12, p. 4204-4208, **DOI:10.1016/j.msea.2011.02.002**.

[49] Zhu, X., Ai, S., Lu, X., Zhu, L., Liu, B. (2014). A novel 3D geometrical reconstruction method for aluminum foams and FEM modeling of the material response. *Theoretical*

and Applied Mechanics Letters, vol. 4, no. 2, p. 021006, **DOI:10.1063/2.1402106**.

[50] Zhu, X., Ai, S., Lu, X., Ling, X., Zhu, L., Liu, B. (2014). Thermal conductivity of closed-cell aluminum foam based on the 3D geometrical reconstruction. *International Journal of Heat and Mass Transfer*, vol. 72, p. 242-249, **DOI:10.1016/j.ijheatmasstransfer.2014.01.006**.

[51] Mankovits, T., Budai, I., Balogh, G., Gábora, A., Kozma, I., Varga, T.A., Manó, S., Kocsis, I. (2014). Structural analysis and its statistical evaluation of a closed-cell metal foam. *International Review of Applied Sciences and Engineering*, vol. 5, no. 2, p. 135-143, **DOI:10.1556/IRASE.5.2014.2.5**.

[52] ASTM E9-09:2009. *Standard Test Methods of Compression Testing of Metallic Materials at Room Temperature*. ASTM International, West Conshohocken, **DOI:10.1520/E0009-09**.

[53] Curle, U.A., Ivanchev, L. (2010). Wear of semi-solid rheocast SiCp/Al metal matrix composites. *Transactions of Nonferrous Metals Society of China*, vol. 20, sup. 3, p. 852-856, **DOI:10.1016/S1003-6326(10)60594-8**.

[54] ISO 13314:2011. *Mechanical Testing of Metals – Ductility Testing – Compression test for Porous and Cellular Metals*. International Organization for Standardization. Geneva.